

# Theoretical Investigation of Coherent Synchrotron Radiation Induced Microbunching Instability in Transport and Recirculation Arcs

C. -Y. Tsai, Virginia Tech, Blacksburg, VA 24061, USA

D. Douglas, R. Li, C. Tennant, Jefferson Lab, Newport News, VA 23606, USA

## ABSTRACT

The coherent synchrotron radiation (CSR) of a high brightness electron beam traversing a system of series of dipoles, such as recirculation or transport arcs, may lead to the microbunching instability. In this presentation, we extend and develop a semi-analytical approach for a general lattice based on the previous formulation with 1-D CSR model [Phys. Rev. ST Accel. Beams 5 064401 (2002)] and apply it to investigate the physical processes of the CSR-induced microbunching instability for two example transport arcs lattices. We find microbunching instability in transport arcs has a distinguishing feature of multistage amplification (up to 6-th stage for our example arcs in contrast to two stage amplification for a 3-dipole chicane). By extending the concept of stage gain as proposed by Huang and Kim [Phys. Rev. ST Accel. Beams 5, 074401 (2002)], we developed a method to quantitatively characterize the microbunching amplification in terms of iterative or staged orders that allows the comparison of optics impacts on microbunching gain for different lattices. The parametric dependencies and Landau damping for our example lattices are also studied in detail. Excellent agreement of the gain functions and spectra from Vlasov analysis with results from ELEGANT is achieved which helps to validate our analyses.

## INTRODUCTION

As is well known, CSR effects have been one of the most challenging issues associated with the designs of magnetic bunch compressor chicane for X-ray FELs and linear colliders. Typically, CSR is emitted not only for wavelength range comparable or longer than the bunch length duration but also for shorter wavelengths if the bunch charge density is modulated at such wavelength range (so called microbunching). Such coherent radiation effects, which had been confirmed both in numerical simulation and experiments, can result in a undesirable beam quality degradation. The above-mentioned works were, however, mostly focused on the studies of magnetic bunch compressor chicanes. Recently the superconducting radio frequency (SRF) energy-recovery linac-based (ERL) facilities (e.g., free-electron laser facility or medium-energy electron-ion collider) have been brought to attention. The recirculation or transport arcs are necessary elements in such facilities. However, similar studies on such systems with multiple modular dipoles as in a transport or recirculation arc were mostly focused on transverse beam dynamics while longitudinal phase space degradation has very limited discussion. In this presentation, we pay attention to the CSR effects on the longitudinal beam dynamics as beam traversing around the recirculation arc, particularly on the CSR-induced microbunching issues. The reasons to be concerned about the microbunching instability are based on the two facts: first, such system is characteristic of long transport lines with many dipole magnets whether in a single or multiple pass operation; the other, the system typically delivers the beam which features high beam quality, i.e. high brightness or low emittance, for the use in next-generation light sources or hadron cooling in high-energy electron recirculating cooling rings. Thus, the seeds, which are derived from either the density ripples from upstream ERL injector or longitudinal space charge especially for low energy transport beam, that cause density modulation would be extremely possible to lead to microbunching instability. Therefore further investigation of CSR-induced effects and its detailed physical processes are of critical importance and may shed light on how to better the future designs for such lattices.

## METHODS

The CSR-induced microbunching gain can be formulated by linearized Vlasov equation in typical bunch compressors [1]. This model is based on the following assumptions and approximations: coasting beam approximation and steady-state 1-D CSR [Derbenev *et al.*, TESLA-FEL-95-05, 1995] with negligible shielding (boundary) effects.

By the method of characteristics, the linearized Vlasov equation can be rewritten as the general form of Volterra integral equation below:

$$(1) \quad g_i(s) = g_i^{(0)}(s) + \int_0^s K(s,s')g_i(s')ds'$$

$$(2) \quad K(s,s') = \frac{ikR_0 C(s)C(s')R_{cs}(s' \rightarrow s)Z(C(s'),s)}{2} \exp\left\{-\frac{kz}{2} \left[ \beta_{cs} R_{cs}(s,s') + \frac{R_{cs}^2(s,s')}{\beta_{cs}} \right] \right\}$$

where the kernel function  $K(s,s')$  describes the CSR interaction,  $g_i(s)$  is the resultant bunching factor as a function of the longitudinal position given the wavenumber  $k$ ,  $g_i^{(0)}(s)$  is the bunching factor without CSR.

In this work, we have extended the formulation to a general transport line by input of the transport functions of a lattice from a common particle tracking code, e.g. ELEGANT [5] and developed a program to solve Eq. (1) self-consistently or Eq. (3) (below) iteratively. Furthermore, we adapt, motivated by [2], the above integral equation by iteratively finding the staged solutions. The advantage of using this method is to facilitate us exploring up to which stage the overall CSR process can be described. The staged iterative solution for  $n$ -th order is defined as

$$(3) \quad g_i^{(n)} = \sum_{m=0}^{n-1} K^{(m)} g_i^{(0)}$$

where we have already expressed the kernel  $K(s,s')$  in matrix form, denoted as  $K$ . It can be easily shown that Eq. (1) and Eq. (2) are equivalent, assuming  $n \rightarrow \infty$  and the sum converges. The CSR-induced microbunching gain is defined as the ratio of the bunching parameter at  $s$  to the initial bunching parameter with some given wave number  $k$ :  $G(s) = |g_i(s)/g_i^{(0)}(0)|$ . Note that  $g_i$  is in general a complex quantity. The stage gain is then  $G^{(n)}(s) = |g_i^{(n)}(s)/g_i^{(0)}(0)|$ .

To compare the CSR gain contributed from individual stage, we further define the *staged gain vector* at the end of a lattice up to a certain order  $M$  as

$$\vec{G}^{(M)} = \vec{G}_0 + \vec{G}_1 I_s + \dots + \vec{G}_M I_s^M = \sum_{n=0}^M \vec{G}_n I_s^n$$

In order to extract the net effect caused by lattice optics, the above expression can be further formulated as

$$(4) \quad \vec{G}^{(M)} = \sum_{n=0}^M A^n d^{(n)} \left( \frac{I_s}{\gamma} \right)^n$$

where  $A = -0.94 + 1.63i$ ,  $I_s$  is the beam current,  $\gamma$  the relativistic factor of beam energy, and  $d^{(n)}$  (given some  $\lambda$ ) now reflects the effects from lattice optics at  $n$ -th stage and Landau damping through beam emittance and energy spread. Final stage gain is  $G^{(M)} = |G^{(M)}(s)| = G^{(M)}(s=s)$ . In the following results,  $\lambda$  is chosen such that it maximizes CSR gain. Here for Example 1 and 2 lattices,  $\lambda_{opt} = 36.82$  and  $19 \mu\text{m}$ , respectively. As mentioned, we implement the above semi-analytical methods (self-consistent and iterative approach) by input of the transport functions from ELEGANT, and then solve Eq. (1) and/or Eq. (3) for the gain function  $G(s)$  or gain spectrum  $G(\lambda)$ .

## SIMULATION RESULTS

### >CSR Microbunching Gain Analysis

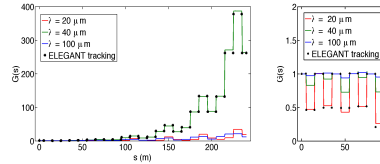


FIG. 1 CSR self-consistent gain functions  $G(s)$  for Example 1 lattice (left) and Example 2 lattice (right) for three different modulation wavelengths.

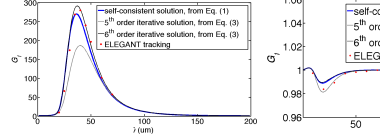


FIG. 2 CSR gain spectra  $G(\lambda)$  as a function of initial wavelength for Example 1 lattice (a) and Example 2 lattice (b). Note the vertical axes are in different scale.

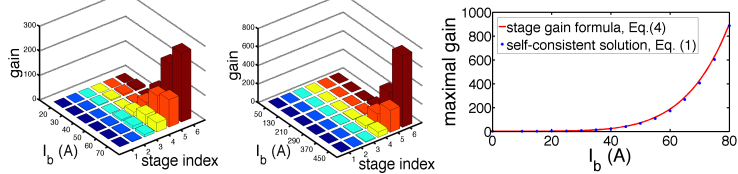


FIG. 3 Bar chart representation of staged gains for several different beam currents for Example 1 (left) and 2 (middle) lattice arcs, where for Example 1 and 2 lattices,  $\lambda_{opt} = 36.82$  and  $19 \mu\text{m}$ , respectively. Note the current scales ( $I_b$ ) are different. (Right) The current dependence of maximal CSR gain for the Example 1 lattice. Solid red line from Eq. (4) with  $M=6$ , and blue dots from Eq. (1).

### > Parametric Dependencies and Landau Damping

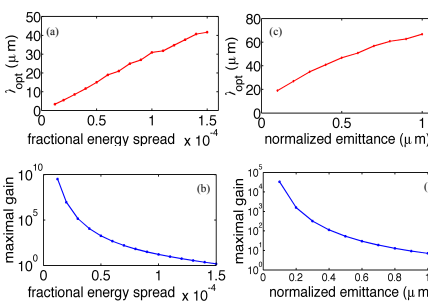


FIG. 4 Optimum wavelength (a, c) and maximal CSR gain (b, d) as a function of beam energy spread with zero emittance (a, b) and finite beam emittance (c, d) with vanishing energy spread.

FIG. 5  $R_{cs}(s' \rightarrow s)$  "quilt" patterns for the two example lattice arcs: (top) Example 1 (bottom) Example 2 for illustration of multi-stage CSR amplification.

## SUMMARY

We extended the previous work [1] and stage-gain concept [2] to study the CSR-induced microbunching gain in transport and recirculation arcs. We found that, different from that of typical bunch compressor chicane, the gain is characteristic of multistage amplifications, e.g. up to 6-th stage in the two example lattices (Figs. 1 and 2). Then we quantified and compared the CSR gains contributed from individual stages for the two lattices (Fig. 3).

The dependence of optimum wavelength and maximal gain on beam energy spread and emittance can be derived [4] from Fig. 4 that

$$\begin{array}{|c|c|c|} \hline \lambda_{opt} \propto & \epsilon_0 = 0 & \sigma_\delta = 0 \\ \hline \sigma_\delta & \sigma_\delta & \sqrt{\epsilon_0} \\ \hline G_{f,max} \propto & \sigma_\delta^{(-4/3)M} & \epsilon_0^{(-2/3)M} \\ \hline \end{array}$$

where  $M$  is the stage order. Whether such numerical observations reflect a general behavior for multistage and arbitrary lattice is still a question for further investigation.

We also demonstrated in Fig. 5 the  $R_{cs}(s' \rightarrow s)$  on the overall CSR gain (also see Eq. (2)) for both example lattices and found that for Example 1 lattice there exist several cumulated large amplitude areas so that the gain eventually add up (i.e. multi-stage amplification) while for Example 2 lattice this situation is well controlled. For the detailed description of the two example lattices, we refer the interested reader to [3].

## REFERENCES

- [1] S. Heifets *et al.*, PRST-AB 5, 064401 (2002)
- [2] Z. Huang and K. Kim, PRST-AB 5, 074401 (2002)
- [3] D. R. Douglas *et al.*, arXiv:1403.2318 or JLAB-ACP-14-1751
- [4] E. L. Saldin *et al.*, NIMA 490, 1 (2002)
- [5] M. Borland, Advanced Photon Source LS-287 (2000)